

Neutrino nonstandard interactions in the supernova

C. R. Das^{*}, João Pulido[†]

CENTRO DE FÍSICA TEÓRICA DE PARTÍCULAS (CFTP)

Departamento de Física, Instituto Superior Técnico

Av. Rovisco Pais, P-1049-001 Lisboa, Portugal

Abstract

Neutrino non-standard interactions (NSI) were investigated earlier in the solar case and were shown to reduce the tensions between the data and the large mixing angle solution predictions. We extend the previous framework to the supernova and evaluate the appearance probabilities for neutrinos and antineutrinos as a function of their energy after leaving the collapsing star with and without NSI. For normal hierarchy the probability for electron neutrinos and antineutrinos at low energy ($E \lesssim 0.8 - 0.9 \text{ MeV}$) is substantially increased with respect to the non-NSI case and joins its value for inverse hierarchy which is constant with energy. Also for inverse hierarchy the NSI and non-NSI probabilities are the same for each neutrino and antineutrino species. Although detection in such a low energy range remains at present an experimental challenge, it will become a visible trace of NSI with normal hierarchy if they exist. On the other hand the neutrino decay probability into an antineutrino and a majoron, an effect previously shown to be induced by dense matter, is, as in the case of the sun, too small to be observed as a direct consequence of NSI.

^{*}E-mail: crdas@cftp.ist.utl.pt

[†]E-mail: pulido@cftp.ist.utl.pt

1 Introduction

Non-standard neutrino oscillations (NSI) [1–9] have since long been applied to solar neutrinos [1, 2, 10] in an attempt to understand the origin of their apparent deficit. More recently interest in NSI has been revived [11, 12] with the purpose of solving the possible inconsistencies between the LMA solution to the solar neutrino problem [13, 14] and the data [15–18]. The most remarkable of these inconsistencies is the absence of any experimental evidence for an upturn in the LMA survival probability in the intermediate energy range of solar neutrinos. It has been shown [11] that NSI can lead to a flat probability in this sector and hence a flat electron energy spectrum as observed in both SuperKamiokande [15] and SNO [17] experiments, with the interesting consequence of a possible neutrino decay into antineutrinos and majorons in dense matter. However, the predicted antineutrino flux is too small to be observed and the only expected signature of the effect is the flatness of the electron spectrum. Extension to supernova neutrinos, which will be done in the present paper, will provide us further information on possible experimental NSI signatures. Our approach to NSI, previously developed in [11] assumes extra contributions to the vertices $\nu_\alpha \nu_\beta$ and $\nu_\alpha e$ and differs therefore from the neutrino-neutrino interaction considered in [7].

The supernova dynamics has been extensively studied and for details we may refer the reader to the review [19]. Here we will just highlight its relevant aspects for our purposes. As is well known when a star of mass $M \gtrsim 8M_\odot$ has burned all its fuel, an onion like structure is formed with the lighter elements in the outer layers and the heavier ones inside. For massive enough stars $M \gtrsim 11M_\odot$ an innermost iron core is formed. Equilibrium of the core is disrupted by photodissociation of the heavier elements producing alpha particles and neutrons. The resulting free electrons are in turn captured by protons and nuclei, producing electron neutrinos which escape,

$$e^- p \rightarrow n \nu_e . \quad (1)$$

When the Coulomb pressure of the electrons becomes insufficient to sustain the core against its own gravity, collapse is initiated until the core becomes no longer transparent to neutrinos and reaches nuclear density ($\rho \simeq 3 \times 10^{14} g cm^{-3}$), a process which takes only about 10 ms [20]. The neutronization process (1) ceases, a state of hydrostatic equilibrium is reached with the core forming a proto-neutron star of radius around 10 km and a temperature of 35-40 MeV. From this stage onwards only thermal neutrinos are emitted. They are produced from nucleon-nucleon bremsstrahlung

$$N N \rightarrow N N \nu \bar{\nu} \quad (2)$$

e^+e^- annihilation,

$$e^+e^- \rightarrow \nu \bar{\nu} \quad (3)$$

plasmon decay,

$$\gamma \rightarrow \nu \bar{\nu} \quad (4)$$

and electron nucleon bremsstrahlung

$$e^- N \rightarrow e^- N \nu \bar{\nu}. \quad (5)$$

So according to core collapse supernova dynamics, in the thermal phase neutrino emission proceeds through all flavour channels and is accompanied by antineutrinos, whereas in the initial neutronization phase only electron neutrinos are expected.

The events observed in SN1987a were all interpreted as antineutrino ones [21] due not only to the dominance of the antineutrino cross section relative to the neutrino one but also possibly to the unavailability of a lower energy threshold, as shall be seen in the present paper. Whether or not any neutrinos reached the Earth is an open question. In ref. [11] it was shown that neutrino decay in dense matter into antineutrinos and a majoron is a necessary consequence of NSI. However its effect through the detection of antineutrinos in the neutronization phase where only ν_e 's are produced is not possible, owing to the smallness of the antineutrino production probability through decay even in the supernova. In fact the high density range of the neutrino trajectory is not long enough to produce a visible antineutrino flux originated from this source.

In this paper we extend for supernova neutrinos the NSI framework that was introduced in the solar neutrino case [11] where it was shown to improve the fits to experiment. In section 2 we review its general features. We recall that a flat SuperKamiokande and SNO electron spectrum necessarily require imaginary diagonal entries in the NSI Hamiltonian. Their real parts, along with the off diagonal entries whether real or imaginary, may be arbitrary in the sense that they do not induce any change in the standard LMA probability. As a consequence neutrino decay in dense matter into an antineutrino and a majoron arises. Section 3 is the main part of our work. Here we extend NSI to the interactions of the supernova neutrinos. We evaluate the survival and conversion probabilities with and without NSI as well as the probability for neutrino decay. For normal mass hierarchy in the absence of NSI the electron neutrino survival probability turns out to be small, most of the ν_e 's having been converted through standard oscillations to ν_μ, ν_τ 's. Furthermore it is found that as in the case of the sun, the decay probability is extremely small for antineutrinos from neutrino decay to ever be observed. Since in the neutronization phase only ν_e 's are produced, no charged current signal is expected to be seen at this initial stage in the absence of NSI. On the other hand in the NSI case a sizeable electron neutrino flux may appear at low energies in the neutronization phase which may be detected through the charged current with improved low energy detectors. At present this remains a challenge but may be reached in the not too distant future. For inverse hierarchy all neutrino fluxes are comparable in the whole energy range. On the other hand in the thermalization phase neutrinos (ν_α) and antineutrinos ($\bar{\nu}_\alpha$) of all kinds are produced so that the initial state is assumed to consist of $\nu_\alpha, \bar{\nu}_\alpha$'s in equal proportions. Owing to the large number of oscillations, the information from the initial state is essentially lost, hence the final probability distributions are the same as in neutronization where only ν_e 's are present initially. The only difference is in this case the obvious presence of antineutrinos with the same probability distribution as

neutrinos due to CPT invariance. Finally in section 4 we comment on our results and draw our conclusions.

2 The NSI Hamiltonian

In this section we highlight and discuss the main steps of the analysis leading to the Hamiltonian for propagation in dense matter (see also [11]). Its results will be used in section 3 for the evaluation of the probabilities for neutrino survival and conversion and the probability for antineutrino production.

Assuming only standard interactions (SI), the potential for electron neutrinos traveling through the sun and supernova is given by

$$V = G_F \sqrt{2} N_e \left(1 - \frac{N_n}{2N_e} \right) = V_c + V_n \quad (6)$$

where N_e , N_n are the electron and neutron density and $V_c = G_F \sqrt{2} N_e$, $V_n = -G_F / \sqrt{2} N_n$. For NSI we assume that the ν_α interaction potential on electrons ($\alpha = e, \mu, \tau$) involves both the charged and neutral currents (CC and NC), while on quarks it involves only NC. NSI give rise to possible lepton flavour violation. Denoting by $\varepsilon_{\alpha\beta}^{fP}$ the NSI factor that multiplies each diagram associated to neutrino propagation in matter we have

$$(v_{\alpha\beta})_{NSI} = G_F \sqrt{2} N_e \left[(\varepsilon_{\alpha\beta}^{eP})_{NC} + \left(-\frac{1}{2} + 2\sin^2\theta_W \right) (\varepsilon_{\alpha\beta}^{eP})_{NC} + \left(1 - \frac{8}{3}\sin^2\theta_W + \frac{N_n}{2N_e} \right) \varepsilon_{\alpha\beta}^{uP} + \left(-\frac{1}{2} + \frac{2}{3}\sin^2\theta_W - \frac{N_n}{N_e} \right) \varepsilon_{\alpha\beta}^{dP} \right] \quad (7)$$

In the following we will assume $(\varepsilon_{\alpha\beta}^{eP})_{CC} = (\varepsilon_{\alpha\beta}^{eP})_{NC}$. Hence flavour change may occur without a vacuum mixing angle [13, 14] or a magnetic moment [22], being induced only by the off diagonal entries of this matrix ($\alpha \neq \beta$). So with SI and NSI the matter Hamiltonian in the flavour basis is the sum of eqs.(6) and (7)

$$\mathcal{H}_M = V_c \begin{pmatrix} 1 & 0 & 0 \\ 0 & 0 & 0 \\ 0 & 0 & 0 \end{pmatrix} + \begin{pmatrix} (v_{ee})_{NSI} & (v_{e\mu})_{NSI} & (v_{e\tau})_{NSI} \\ (v_{\mu e})_{NSI} & (v_{\mu\mu})_{NSI} & (v_{\mu\tau})_{NSI} \\ (v_{\tau e})_{NSI} & (v_{\tau\mu})_{NSI} & (v_{\tau\tau})_{NSI} \end{pmatrix} = \mathcal{H}_{SI} + \mathcal{H}_{NSI} . \quad (8)$$

As is well known, owing to the large neutrino density, collective effects can play an important role in the supernova [23], [24], [25][‡], providing an additional contribution to the matrix (8). They occur up to a few 100 km, whereas MSW oscillations occur typically at larger distances so that MSW effects factorize and can be included separately [27]. For this reason the NSI effects, intrinsically associated to MSW, must also be included separately. We will perform

[‡]For a review on collective oscillations see [26].

our calculation starting from a region around 400-500 km where collective oscillations have already taken place. Hence their net effect to our approach amounts to the well known spectral swap-split of the neutrino and antineutrino energy spectra [24], [25], [28]. However it was recently shown that matter completely suppresses collective oscillations up to 200 ms [29] after bounce. In view of these results it appears that collective effects can be ignored at early times in a supernova. Our results, derived in the next section, are therefore expected to be valid for the whole neutronization phase and part of the subsequent thermal phase.

The investigation performed in ref. [11] shows that no off diagonal entry in matrix (8) whether real or imaginary, can change the LMA probability, hence the rates and the corresponding SuperKamiokande and SNO electron spectra. In fact only imaginary diagonal couplings lead to a change in P_{LMA} . As discussed in ref. [11], this implies the instability of neutrinos in matter and their decay into antineutrinos of all species along with majorons. Requiring the convenient change in P_{LMA} , namely the one that leads to a flat electron spectrum in SuperKamiokande and SNO, thus allowing for imaginary diagonal couplings, it was shown that the simplest choice of parameters is

$$\mathcal{H}_{NSI} = G_F \sqrt{2} N_e \left[\begin{pmatrix} \frac{i}{2}\varepsilon(x_e + 1) & & \\ & -i\varepsilon x_e & \\ & & \frac{i}{2}\varepsilon x_e \end{pmatrix} + x_u \begin{pmatrix} \frac{i}{2}\varepsilon & & \\ & -i\varepsilon & \\ & & \frac{i}{2}\varepsilon \end{pmatrix} + x_d \begin{pmatrix} -\frac{i}{2}\varepsilon & & \\ & i\varepsilon & \\ & & -\frac{i}{2}\varepsilon \end{pmatrix} \right] \quad (9)$$

with vanishing off diagonal entries and $\varepsilon = 3.5 \times 10^{-4}$. Here

$$x_e = -\frac{1}{2} + 2\sin^2\theta_W, \quad x_u = 1 - \frac{8}{3}\sin^2\theta_W + \frac{N_n}{2N_e}, \quad x_d = -\frac{1}{2} + \frac{2}{3}\sin^2\theta_W - \frac{N_n}{N_e}. \quad (10)$$

The three matrices in the right hand side of eq. (9) relate to the neutrino interaction with electrons, u-quarks and d-quarks respectively. Each diagonal entry refers to the ν_e , ν_μ , ν_τ contribution to its own interaction, hence its decay. So for instance, for ν_e the NSI (decay) potential is

$$(v_{ee})_{NSI} = \frac{i}{2}\varepsilon G_F \sqrt{2} N_e (x_e + 1 + x_u - x_d). \quad (11)$$

In this way we obtain the three interaction (decay) potentials

$$(v_{ee})_{NSI} = iG_F \sqrt{2} (3.5 \times 10^{-4}) N_e \left(1 - \frac{2}{3}\sin^2\theta_W + \frac{3N_n}{4N_e} \right) \quad (12)$$

$$(v_{\mu\mu})_{NSI} = iG_F \sqrt{2} (3.5 \times 10^{-4}) N_e \left(-1 + \frac{4}{3}\sin^2\theta_W - \frac{3N_n}{2N_e} \right) \quad (13)$$

$$(v_{\tau\tau})_{NSI} = \frac{i}{2}G_F \sqrt{2} (3.5 \times 10^{-4}) N_e \left(1 - \frac{4}{3}\sin^2\theta_W + \frac{3N_n}{2N_e} \right). \quad (14)$$

The full Hamiltonian including the vacuum part and referred to the mass basis is now

$$\mathcal{H} = \begin{pmatrix} 0 & 0 & 0 \\ 0 & \frac{\Delta m_{21}^2}{2E_0} & 0 \\ 0 & 0 & \frac{\Delta m_{31}^2}{2E_0} \end{pmatrix} + U^\dagger \mathcal{H}_M U \quad (15)$$

with \mathcal{H}_M given by (8) with the replacements (12), (13), (14) and arbitrary off diagonal entries. In eq. (15) Δm_{21}^2 , Δm_{31}^2 are the solar and atmospheric mass differences, U is the PMNS matrix [30] defined with the standard parameterisation [31] and we use the central value for $\sin\theta_{13} = 0.13$ from ref. [13]. The negative imaginary parts of the eigenvalues of (15) are the mass eigenstate decay rates Γ_i which will be used in the next section for the evaluation of the probabilities. As for the supernova parameters, numerical simulations [32] yield the electron number density and supernova density profiles which in our period of interest (the initial 200 ms) are well approximated by

$$Y_e = \frac{1}{3} - 0.04 \log \frac{\rho}{10^{12} g \text{ cm}^{-3}} \quad (16)$$

$$\rho = \rho_0 \left(\frac{10 \text{ km}}{r} \right)^3 g \text{ cm}^{-3} \quad (17)$$

for $r > 10 \text{ km}$ with $\rho_0 \sim 10^{14} g \text{ cm}^{-3}$ and which will be used in the next section.

3 Rates, couplings and probabilities

3.1 Rates and neutrino majoron couplings

The ν_e flux from neutronization is in fact a linear combination of the three mass eigenstates ν_i displayed in fig.1(a) for neutrino energy $E_0 = 11 \text{ MeV}$ and normal hierarchy. Our first purpose in this section is to evaluate the decay rate of the NSI process [33–38]

$$\nu_i \rightarrow \bar{\nu}_j + \chi \quad (18)$$

where χ denotes the majoron. This rate satisfies [11], [37]

$$\frac{\partial \Gamma_i}{\partial E_f} = \sum_{j=1}^3 \frac{|g_{ij}|^2}{8\pi} \frac{E_0 - E_f}{E_0^2} |v_i(r) - \bar{v}_j(r)|_{NSI} F(r, E_0) \quad (19)$$

where g_{ij} are the neutrino majoron couplings [37], [38] and the interaction potentials satisfy in the mass basis $v_i = -\bar{v}_i$. Here E_0 is the initial neutrino energy, E_f is the antineutrino energy which in a first approximation we assume to take values in the interval $(0, E_0)$, since

the energy E_0 is shared by the final neutrino and the majoron. The quantity $F(E_0, r)$ is the Fermi factor [37]

$$F(E_0, r) = \left(1 - \frac{1}{e^{(E_0 - \mu)/T} + 1} \right), \quad (20)$$

which reflects the fact that inside the supernova some of the states have already been occupied by neutrinos. In the inner core ($R_{inner} \simeq 10 \text{ km}$) the chemical potential for ν_e (μ_{ν_e}) is around 200 MeV and the temperature $T = 35 \text{ MeV}$. In the outer core ($R_{inner} \simeq 15 \text{ km}$) the temperature drops abruptly $T = 2 \text{ MeV}$, the density falls from $5 \times 10^{14} \text{ g cm}^{-3}$ to $5 \times 10^{13} \text{ g cm}^{-3}$ and we may set $\mu_{\nu_e} = 0$. Hence in the following we will omit the factor $F(E_0, r)$.

The three decay rates Γ_i are the imaginary parts of the NSI Hamiltonian eigenvalues. They are represented in fig.1(b) for $E_0 = 11 \text{ MeV}$. As in the solar case, only Γ_3 is negative, so only the state ν_3 is unstable, allowing for the decay into either $\bar{\nu}_1$, $\bar{\nu}_2$ or $\bar{\nu}_3$, thus generating antineutrinos of the three flavours. One could obtain an alternative expression for $\Gamma_i(r, E_0)$ through the integration of equation (19) over E_f

$$\Gamma_i = \int_0^{E_0} \frac{\partial \Gamma_i}{\partial E_f} dE_f = \sum_{j=1}^3 \frac{|g_{ij}|^2}{16\pi} |v_i(r) - \bar{v}_j(r)|. \quad (21)$$

The vanishing lower limit used in this integration is as referred to above only an approximation, since the majoron obtains a tiny effective mass in matter $m_{eff}^2 \sim |g|^2 N_\nu / q$ [37]. In this way a slight dependence of the rate Γ_i on E_0 arises which is consistent with the numerical evaluation of the imaginary part of the NSI Hamiltonian eigenvalues.

The parameters $\varepsilon_{\alpha\beta}$ were fixed earlier (see section 2) by the fittings to the solar neutrino data [11] and so the rates $\Gamma_i(r, E_0)$, numerically evaluated as the imaginary parts of the Hamiltonian eigenvalues, are also fixed. Moreover the values of g_{ij} to which the rates correspond are so far unknown and only upper bounds exist in the literature [38]. In the following we will use the strictest one quoted, namely

$$\sum_{\alpha} |g_{e\alpha}|^2 < 5.5 \times 10^{-6}, \quad (22)$$

conveniently expressed in the mass basis. Quantities Γ_i will now be used in the evaluation of the probabilities.

3.2 Probability densities for neutrino survival, decay and antineutrino appearance

We denote by $P_{\nu_i}(r, E_0)$ the ν_i survival probability in the mass basis for neutrino energy E_0 at a distance r from the star centre, obtained from integration of the Schrödinger equation with the Hamiltonian (15), and by $\phi_{\nu_e}(E_0)$ the initial normalized neutrino spectral flux [20]

$$\phi_{\nu_e}(E_0) = \frac{1}{\Phi(E_0)} \frac{\partial \Phi}{\partial E_0}.$$

Given these definitions the quantity

$$\phi_{\nu_i}(r, E_0) = P_{\nu_i}(r, E_0) \phi_{\nu_e}(E_0) \quad (23)$$

is the normalized spectral flux of ν_i mass eigenstates with energy E_0 that remain in the beam after traveling a distance r . Hence

$$\frac{\partial P_{\nu_i^m}(E_0)}{\partial r} = \int_0^{E_0} \phi_{\nu_i}(r, E_0) (1 - e^{\Gamma_i(r, E_0)r}) \frac{\partial \Gamma_i(r, E_0, E_f)}{\partial E_f} dE_f \quad (24)$$

is the probability per unit star radius for this mass eigenstate to have disappeared from the flux.

Replacing now (19) in (24) one obtains the probability for the ν_i mass eigenstate disappearance

$$P_{\nu_i^m}(E_0) = \sum_{j=1}^3 \frac{|g_{ij}|^2}{8\pi} \int_{R_i}^{R_S} |v_i(r) - \bar{v}_j(r)|_{NSI} \phi_{\nu_i}(r, E_0) (1 - e^{\Gamma_i(r, E_0)r}) \int_0^{E_0} \frac{E_0 - E_f}{E_0^2} dE_f dr \quad (25)$$

Quantities R_i and R_S denote the neutrino sphere and the star radii respectively. We note that in eq.(25) we have the simple sum of probabilities, since each eigenstate ν_i , as it decays, can give rise to just one antineutrino flavour which is a linear combination of the three mass eigenstates ν_j . Performing the integration in E_f , (25) can be simplified to

$$P_{\nu_i^m}(E_0) = \sum_{j=1}^3 \frac{|g_{ij}|^2}{16\pi} \int_{R_i}^{R_S} |v_i(r) - \bar{v}_j(r)|_{NSI} \phi_{\nu_i}(r, E_0) (1 - e^{\Gamma_i(r, E_0)r}) dr. \quad (26)$$

In other words, given a flux of ν_i 's with an energy in the interval $[E_0, E_0 + dE_0]$, the quantity $P_{\nu_i^m}(E_0)dE_0$ is the fraction of these neutrinos which has decayed into antineutrinos with an energy in the interval $(0, E_0 + dE_0)$ after traversing the star. The fraction of ν_i 's that remains in the beam after leaving the star is $P_{\nu_i}(R_S, E_0)dE_0$ with $P_{\nu_i}(r, E_0)$ as defined in the beginning of this section (see (23)).

As a reminder we note that the normalization of P_{ν_i} follows from

$$P_{\nu_i} = |< \nu_i | \nu_e >|^2 = |\nu_i u_{ej}^* \nu_j|^2 = u_{ej}^* u_{ek} \nu_j \nu_k \nu_i \nu_i = u_{ej}^* u_{ek} \delta_{ij} \delta_{ik} = u_{ei}^* u_{ei} \quad (27)$$

(no sum over i) with the orthogonality of U^{PMNS} ensuring $\sum_i P_{\nu_i} = 1$. Moreover the integration of the equation of motion proceeds in the mass basis, so that the normalization condition is forced on P_{ν_i} . The normalization of P_{ν_α} also follows in a similar way

$$\begin{aligned} P_{\nu_\alpha} &= |< \nu_\alpha | \nu_e >|^2 = |u_{\alpha i}^* u_{ej} \nu_i \nu_j|^2 = u_{\alpha i}^* u_{ej}^* u_{\alpha k} u_{em} \nu_i \nu_j \nu_k \nu_m \\ &= u_{\alpha i}^* u_{ej}^* u_{\alpha j} u_{ei} = \delta_{\alpha e} u_{\alpha i}^* u_{ei} \end{aligned} \quad (28)$$

(no sum over α) with the orthogonality of U^{PMNS} implying $\sum_\alpha P_{\nu_\alpha} = 1$. In (27) and (28) we neglected the plane wave propagation phases. Finally the flavour probability is obtained from

$$P_{\nu_\alpha} = |u_{\alpha i} < \nu_i | \nu_e >|^2 \quad (29)$$

and is shown in fig.2 for standard ($\varepsilon = 0$) and non-standard interactions ($\varepsilon = 3.5 \times 10^{-4}$).

For the sake of the following discussion we recall that from supernova theory only electron neutrinos are produced in the initial neutronization phase. From fig.2 with normal hierarchy (panel (a)) it is seen that, in the absence of NSI, electron neutrinos can hardly be detected, as the survival probability is around 0.02 and practically constant with energy. Further, ν_μ 's and ν_τ 's produced from oscillations, although having a much larger production probability (~ 0.5), can only be detected through neutral current reactions, so there will be no way to distinguish them at present from other neutrinos or antineutrinos. The major difference in the NSI case for normal hierarchy as seen from fig.2a is the appearance of a visible flux of electron neutrinos in the low energy region ($E_0 \lesssim 0.8 - 0.9 \text{ MeV}$). This can be pinpointed in the neutronization phase through the charged current, provided enough experimental capability is developed in the future to reduce the low energy threshold. On the other hand for inverse hierarchy (fig.2b) no difference appears between NSI and non-NSI: the sizable value of the ν_e probability (~ 0.31) is the same at low energy as in the normal hierarchy case and remains constant with energy, so ν_e detection is experimentally accessible. However the NSI and non-NSI probability values are the same for each neutrino species and also remain in each case constant with energy. So for inverse hierarchy NSI and non-NSI appear indistinguishable.

We next investigate the possibility for electron antineutrinos to be detected in the initial neutronization phase. As previously referred, only electron neutrinos are produced at this stage in a 10 ms pulse. Their decay in matter into electron antineutrinos in a significant number would provide a clear signature of NSI in this initial pulse. Antineutrinos with energy E_f are produced from electron neutrino decay with energy E_0 in the interval $(E_f, E_{0max}]$. Their appearance probability density is in the mass basis

$$P_{\bar{\nu}_j}(E_f) = \bigcup_{i=1}^3 \frac{|g_{ij}|^2}{8\pi} \int_{R_i}^{R_s} |v_i(r) - \bar{v}_j(r)|_{NSI} \int_{E_f}^{E_{0max}} \phi_{\nu_i}(r, E_0) (1 - e^{\Gamma_i(r, E_0)r}) \frac{E_0 - E_f}{E_0^2} dE_0 dr. \quad (30)$$

Contrary to eq.(26), where each neutrino could decay into one *single* antineutrino, each antineutrino can be now produced from more than one neutrino, hence the reason to consider the union of events in eq.(30) [§]. Assuming CPT invariance the flavour probability for $\bar{\nu}_e$ is given by

$$P_{\bar{\nu}_e} = |u_{ei}|^2 P_{\bar{\nu}_i}. \quad (31)$$

Using the bound (22) as a common value for all neutrino majoron couplings involved, we obtain the result displayed in fig.3 for $P_{\bar{\nu}_e}$ which is obviously too small for $\bar{\nu}_e$'s to be observed. If one considers the ν_e decay into $\bar{\nu}_\tau$ one may relax (22) and use instead [38]

$$\sum_{\alpha} |g_{\tau\alpha}|^2 < 5.5 \times 10^{-2} \quad (32)$$

[§]The probability for the union of three independent events (A_1, A_2, A_3) is given by the well known rule $P(A) = P(A_1) + P(A_2) + P(A_3) - P(A_1)P(A_2) - P(A_1)P(A_3) - P(A_2)P(A_3) + P(A_1)P(A_2)P(A_3)$.

as a common value for all couplings. In this case the uppermost value of the probability is raised by a factor $O(10^4)$ which is still too small for the effect to be observed and moreover $\bar{\nu}_e$'s, if produced from ν_τ decay, would appear as a higher order effect. On the other hand, as pointed above, the ν_e probability from oscillations in the absence of NSI is seen to be rather small in normal hierarchy (fig.2a). The prospects for its detection and hence a charged current signal in the neutronization phase will crucially depend on the detector size and supernova distance. With NSI, it may become clearer through $\nu_e d \rightarrow p p e^-$ or an increased $\nu e^- \rightarrow \nu e^-$ scattering event rate, however at low energy ($E_0 \lesssim 0.8 - 0.9 \text{ MeV}$), which is still an experimental challenge. For inverse hierarchy, as also pointed above, the situation is much different: the ν_e signal appears louder and clearer (see fig.2b).

In the subsequent thermalization phase $\bar{\nu}_e$'s and $\nu_X, \bar{\nu}_X$'s with $X = \mu, \tau$ are produced initially along with ν_e 's. All kinds of neutrinos and antineutrinos will arise from these through NSI. The appearance probability for antineutrinos from neutrino decay may increase substantially, since the bound (32) must now obviously be taken into account instead of (22). Again this is not expected to be enough for the effect to be observable (see fig.3) even for $\bar{\nu}_e$ appearance, despite the higher rate involved in its detection. As for the other probabilities from oscillations and NSI, they must be evaluated from the union of events as in (30), since each final neutrino or antineutrino is produced simultaneously from a number of different initial ones. Evaluating these probabilities taking into account their normalization, it turns out that the contribution from the extra initial neutrinos and antineutrinos does not change their value nor energy distribution relative to the neutronization case when initially only ν_e 's are present. In fact the information from the initial state is lost due to the exceedingly large number of oscillations that the neutrinos undergo during propagation: only the propagation physics which depends on the interaction potentials is relevant here. Thus the same fig.2 applies for thermalization both for normal and inverse hierarchies. The only notorious characteristic to tell NSI from non-NSI is, as in neutronization and normal hierarchy, the comparatively large probability for $\nu_e, \bar{\nu}_e$ at low energy ($E_0 \lesssim 0.8 - 0.9 \text{ MeV}$) with the same energy profile. Such low energy raises however an experimental challenge for detection. For inverse hierarchy ν_e 's and $\bar{\nu}_e$'s remain equally abundant both for $E_0 \lesssim 0.8 - 0.9 \text{ MeV}$ and larger, therefore their detection is accessible, although NSI and non-NSI are indistinguishable in this case (see fig.2b). In particular $\bar{\nu}_e$'s provide a clear signal through the reaction $\bar{\nu}_e p \rightarrow n e^+$ whose cross section is $O(10^2)$ larger than for scattering with electrons. Since thermalization is a much longer process than neutronization ($>10 \text{ s}$), a larger accumulation of events is possible in this phase.

For the detection and measurement of the $\nu_\mu, \bar{\nu}_\mu, \nu_\tau, \bar{\nu}_\tau$ individual energy spectra which can only be traced via neutral currents, an interesting proposal was presented some time ago [39] and recently revived [40]. It is based on the $\nu p \rightarrow \nu p$ scattering reaction which can be observed in scintillator detectors (e.g. Borexino, SNO+, KamLAND) through their adequate preparation. This is a neutral current process with a cross section about $O(10^2)$ larger than neutrino electron scattering at supernova neutrino energies. For the NSI scenario expound in the present paper this technique will be particularly useful, since it appears to

be possible to clearly distinguish between normal and inverted hierarchies. In fact it suffices to note that for normal hierarchy the above mentioned neutrinos arrive copiously on Earth in comparison with the more rare ν_e 's and $\bar{\nu}_e$'s whereas for inverse hierarchy all species arrive in comparable numbers (see fig.2a, b).

4 Summary and conclusions

We have extended to the supernova the previously developed model for neutrino NSI in the sun introduced earlier to remove the tension between the LMA predictions and the experimental signatures of solar neutrinos, especially the absence of an upturn in the SuperKamiokande event rate. Improving the data fittings in the solar case implies neutrino decay in dense matter into antineutrino and a majoron, hence the motivation to investigate the consequences of the model for the supernova.

In the present paper we found however that, although the matter density in supernova is much larger than in the sun, the extension of neutrino trajectory in the very high density medium is too short to imply a significant neutrino decay into antineutrino and a majoron and the corresponding appearance probability is insignificant. In the initial and short neutronization phase (10 ms) where only neutrinos are produced through the reaction (1) no antineutrinos are expected experimentally whether or not NSI applies. The important NSI trace is the ν_e appearance probability which increases from 0.02 to 0.31 at low energies ($E_0 \lesssim 0.8 - 0.9 \text{ MeV}$) for normal hierarchy, while for inverse hierarchy NSI and non-NSI cannot be distinguished. In this case the ν_e probability remains at 0.31 regardless of the energy. In the neutronization (deleptonization) phase ν_e 's are the only states that can induce charged current interactions, so they can be singled out either through an increased $\nu e^- \rightarrow \nu e^-$ scattering event rate or $\nu_e d \rightarrow p p e^-$. The remainder (ν_μ 's, ν_τ 's) inducing only neutral currents, cannot be distinguished from each other nor from ν_e 's. Detecting these ν_e 's remains however an experimental challenge at present in normal hierarchy, but not so for inverse hierarchy, as they appear more copiously at higher energies. In the subsequent and longer thermalization phase, the extra neutrino and antineutrino states ($\bar{\nu}_e$ and $\nu_X, \nu_{\bar{X}}$ with $X = \mu, \tau$) that are produced through processes (2)-(5) cannot change the appearance probabilities relative to the neutronization phase. Hence detecting these ν_e 's and $\bar{\nu}_e$'s is, again, an experimental challenge in normal hierarchy: as for the neutronization phase ν_e 's can be detected through a major event rate increase originated from the charged current in $\nu e^- \rightarrow \nu e^-$ scattering or through the reaction $\nu_e d \rightarrow p p e^-$, while $\bar{\nu}_e$'s through the clear signal $\bar{\nu}_e p \rightarrow n e^+$. The remaining neutrinos and antineutrinos can only be detected through the neutral current and so cannot be distinguished from ν_e 's and $\bar{\nu}_e$'s, unless the interesting technique proposed in [39], [40] is developed. If and when this advancement succeeds, it may be possible within the present scenario to tell normal from inverse hierarchy. As regards collective oscillations, their effect in our analysis amounts to the modification of the neutrino and antineutrino spectral fluxes. Collective effects are however probably suppressed up to 0.2 seconds after bounce. The results obtained are therefore applicable to the neutronization

(deleptonization) phase and part of the subsequent thermal phase.

To summarize, in the presence of NSI we expect a sizable flux of ν_e 's and $\bar{\nu}_e$'s at all energies for inverse hierarchy and at low energy ($E_0 \lesssim 0.8 - 0.9 \text{ MeV}$) for normal hierarchy. These fluxes are the same as for non-NSI. The clear distinction between NSI and non-NSI is possible only for normal hierarchy at low energy with a more intense flux of ν_e and $\bar{\nu}_e$, whose detection is at present an experimental challenge. Hence in the absence of NSI the chances for observation in normal hierarchy of a charged current signal do not appear much favourable at present, but they will of course mainly depend on the detector size and supernova distance. Other neutrinos and antineutrinos are in contrast abundantly present, however they can only be detected through the neutral current. As in the case of the sun the antineutrino appearance probability from NSI neutrino decay is in all cases too small for antineutrinos to be detected from this origin.

References

- [1] M. M. Guzzo, A. Masiero and S. T. Petcov, Phys. Lett. B **260** (1991) 154.
- [2] E. Roulet, Phys. Rev. D **44**, 935 (1991).
- [3] Y. Grossman, Phys. Lett. B **359**, 141 (1995) [arXiv:hep-ph/9507344].
- [4] L. M. Johnson and D. W. McKay, Phys. Rev. D **61** (2000) 113007 [arXiv:hep-ph/9909355].
- [5] P. Huber and J. W. F. Valle, Phys. Lett. B **523**, 151 (2001) [arXiv:hep-ph/0108193].
- [6] P. Huber, T. Schwetz and J. W. F. Valle, Phys. Rev. D **66**, 013006 (2002) [arXiv:hep-ph/0202048].
- [7] M. Blennow, A. Mirizzi and P. D. Serpico, Phys. Rev. D **78** (2008) 113004 [arXiv:0810.2297 [hep-ph]].
- [8] C. Biggio, M. Blennow and E. Fernandez-Martinez, JHEP **0908**, 090 (2009) [arXiv:0907.0097 [hep-ph]].
- [9] C. Wei, Phys. Rev. D **82**, 016008 (2010) [arXiv:1003.1468 [hep-ph]].
- [10] J. Pulido, Mod. Phys. Lett. A **8** (1993) 1273.
- [11] J. Pulido and C. R. Das, Phys. Rev. D **83** (2011) 053009 [arXiv:1012.3842 [hep-ph]].
- [12] A. Palazzo, Phys. Rev. D **83** (2011) 101701 [arXiv:1101.3875 [hep-ph]].
- [13] G. L. Fogli *et al.*, Phys. Rev. D **78**, 033010 (2008) [arXiv:0805.2517 [hep-ph]].

- [14] T. Schwetz, M. A. Tortola and J. W. F. Valle, New J. Phys. **10**, 113011 (2008) [arXiv:0808.2016 [hep-ph]].
- [15] J. P. Cravens *et al.* (Super-Kamiokande Collaboration), Phys. Rev. D **78**, 032002 (2008) [arXiv:0803.4312 [hep-ex]].
- [16] Michael B. Smy (Super-Kamiokande Collaboration), J. Phys. Conf. Ser. **203**, 012082 (2010).
- [17] B. Aharmim *et al.* (SNO Collaboration), Phys. Rev. C **81**, 055504 (2010) [arXiv:0910.2984 [nucl-ex]].
- [18] G. Bellini *et al.* (Borexino Collaboration), Phys. Lett. B **696**, 191 (2011) arXiv:1010.0029 [hep-ex].
- [19] S. M. Bilenky, C. Giunti, J. A. Grifols and E. Masso, Phys. Rept. **379** (2003) 69 [arXiv:hep-ph/0211462].
- [20] T. A. Thompson, A. Burrows and P. A. Pinto, Astrophys. J. **592** (2003) 434 [arXiv:astro-ph/0211194].
- [21] K. Sato and H. Suzuki, Phys. Rev. Lett. **58** (1987) 2722.
- [22] C. R. Das, J. Pulido and M. Picariello, Phys. Rev. D **79**, 073010 (2009) [arXiv:0902.1310 [hep-ph]].
- [23] S. Pastor and G. Raffelt, Phys. Rev. Lett. **89** (2002) 191101 [arXiv:astro-ph/0207281].
- [24] H. Duan, G. M. Fuller, J. Carlson, Y. -Z. Qian, Phys. Rev. Lett. **97** (2006) 241101. [astro-ph/0608050].
- [25] H. Duan, G. M. Fuller, J. Carlson, Y. -Z. Qian, Phys. Rev. **D74** (2006) 105014. [astro-ph/0606616].
- [26] H. Duan, G. M. Fuller, Y. -Z. Qian, Ann. Rev. Nucl. Part. Sci. **60** (2010) 569-594. [arXiv:1001.2799 [hep-ph]].
- [27] B. Dasgupta, A. Dighe, Phys. Rev. **D77** (2008) 113002. [arXiv:0712.3798 [hep-ph]].
- [28] B. Dasgupta, A. Dighe, G. G. Raffelt, A. Y. Smirnov, Phys. Rev. Lett. **103** (2009) 051105. [arXiv:0904.3542 [hep-ph]].
- [29] S. Chakraborty, T. Fischer, A. Mirizzi, N. Saviano, R. Tomas, Phys. Rev. Lett. **107** (2011) 151101. [arXiv:1104.4031 [hep-ph]].
- [30] Z. Maki, M. Nakagawa and S. Sakata, Prog. Theor. Phys. **28**, 870 (1962).
- [31] C. Amsler *et al.* (Particle Data Group), Phys. Lett. B **667**, 1 (2008).

- [32] T. Fischer, S. C. Whitehouse, A. Mezzacappa, F. K. Thielemann and M. Liebendorfer, *Astron. Astrophys.* **517** (2010) A80 [arXiv:0908.1871 [astro-ph.HE]].
- [33] Z. G. Berezhiani, M. I. Vysotsky, *Phys. Lett.* **B199** (1987) 281.
- [34] Z. G. Berezhiani, A. Y. Smirnov, *Phys. Lett.* **B220** (1989) 279-284.
- [35] M. Kachelriess, R. Tomas and J. W. F. Valle, *Phys. Rev. D* **62**, 023004 (2000) [arXiv:hep-ph/0001039].
- [36] R. Tomas, H. Pas and J. W. F. Valle, *Phys. Rev. D* **64**, 095005 (2001) [arXiv:hep-ph/0103017].
- [37] Y. Farzan, *Phys. Rev. D* **67**, 073015 (2003) [arXiv:hep-ph/0211375].
- [38] A. P. Lessa and O. L. G. Peres, *Phys. Rev. D* **75**, 094001 (2007) [arXiv:hep-ph/0701068].
- [39] J. F. Beacom, W. M. Farr, P. Vogel, *Phys. Rev.* **D66** (2002) 033001. [hep-ph/0205220].
- [40] B. Dasgupta, J. F. Beacom, *Phys. Rev.* **D83** (2011) 113006. [arXiv:1103.2768 [hep-ph]].

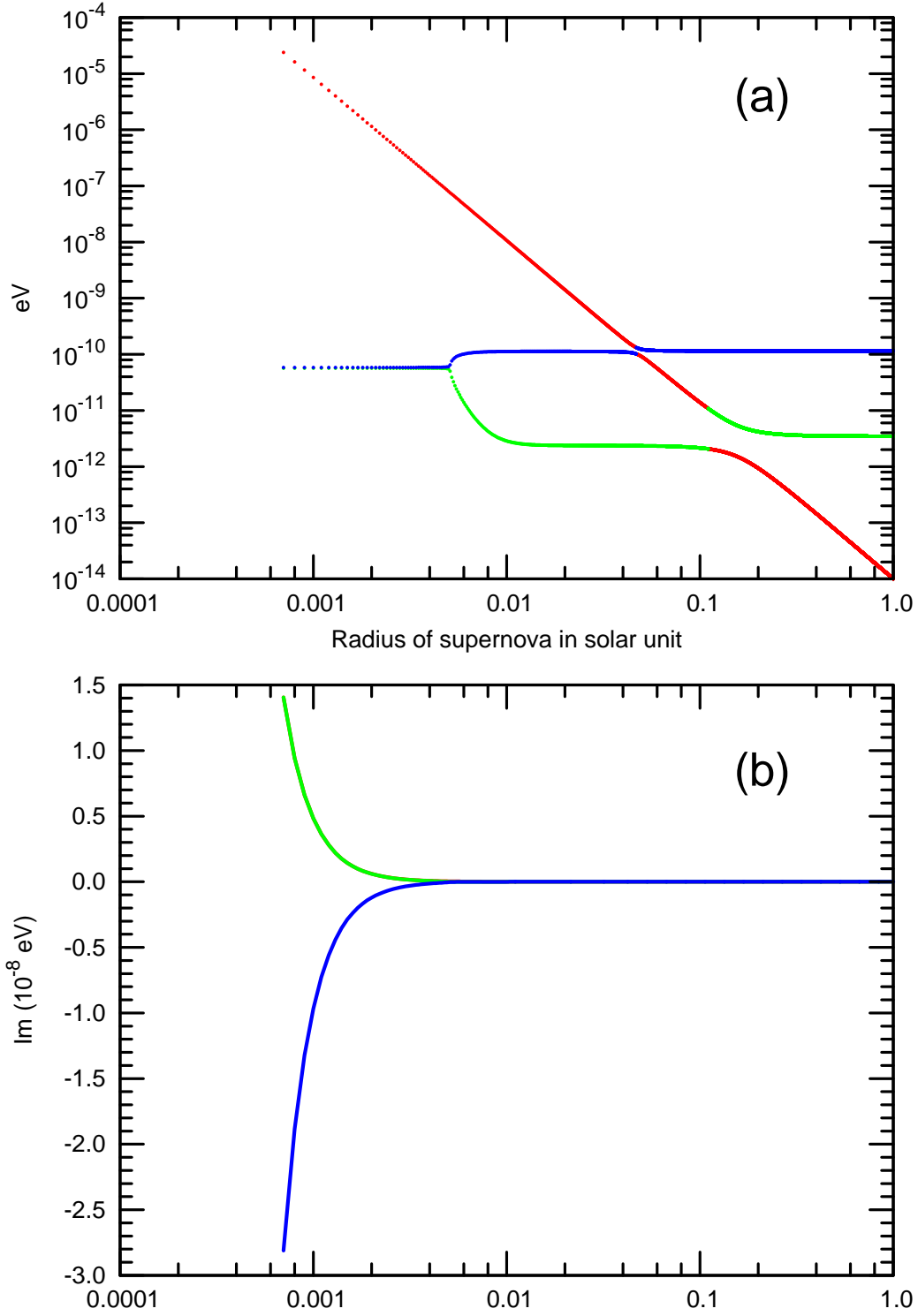


Figure 1: The real (a) and imaginary parts (b) of the neutrino mass matter eigenvalues for neutrino energy $E_0 = 11\text{MeV}$. The two resonances ('atmospheric' and 'solar') are clearly visible in panel (a) and the two positive imaginary parts are superimposed in panel (b).

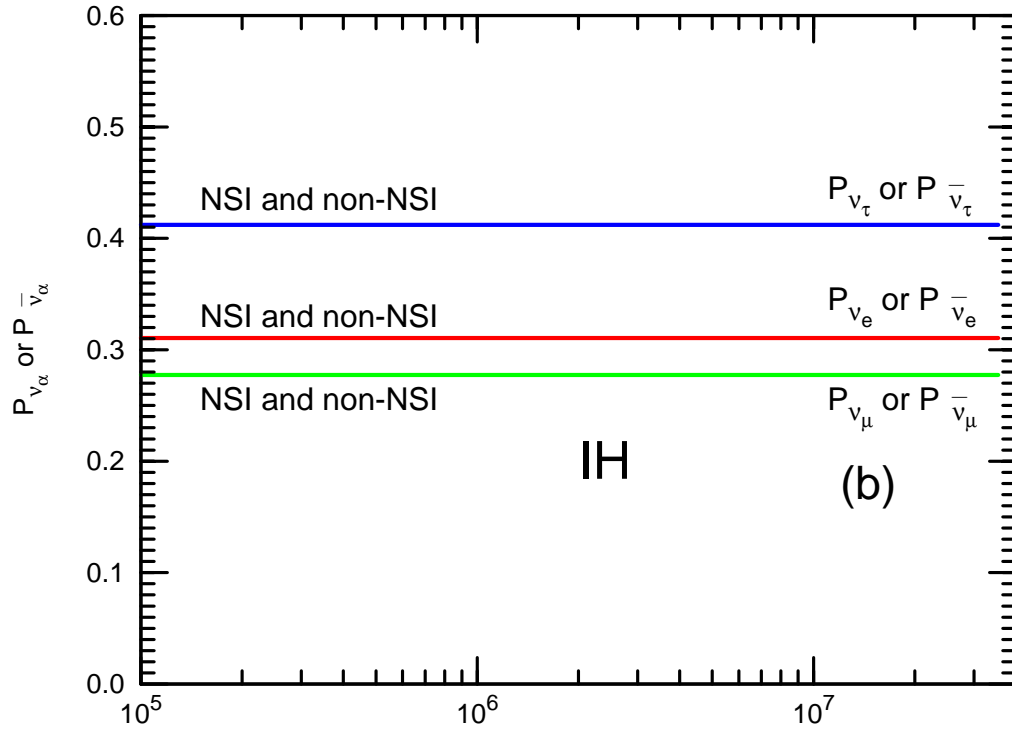
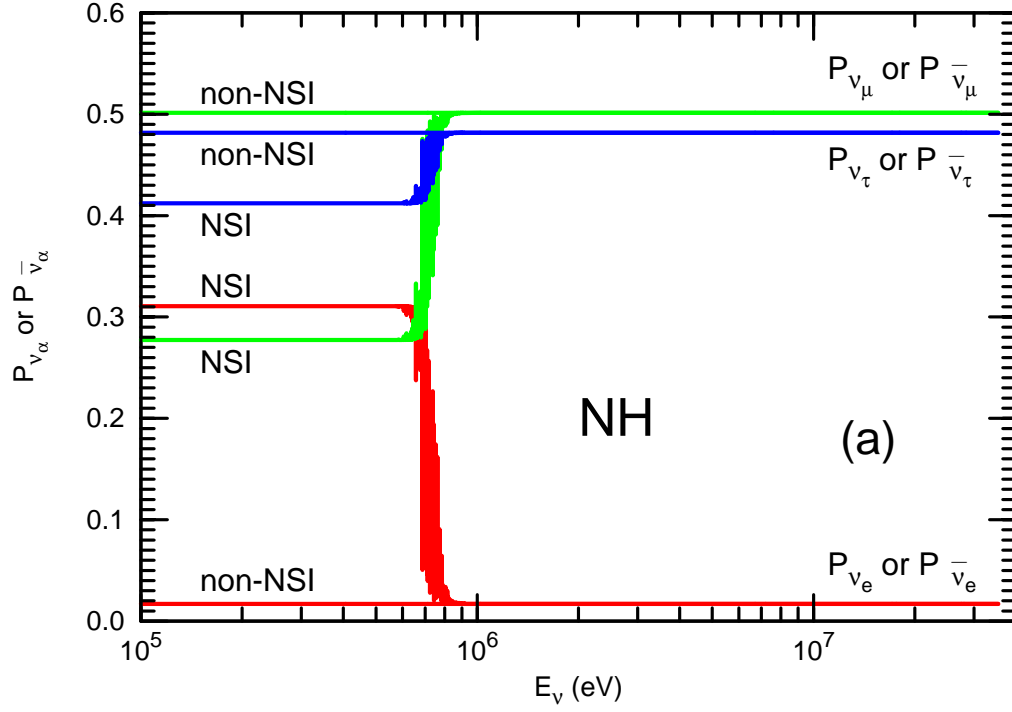


Figure 2: The appearance probabilities P_{ν_e} , $P_{\bar{\nu}_e}$, P_{ν_μ} , $P_{\bar{\nu}_\mu}$, P_{ν_τ} , $P_{\bar{\nu}_\tau}$ with and without NSI ((a) normal hierarchy, (b) inverse hierarchy). For normal hierarchy and energy below 0.9 MeV the NSI probability merges with its non-NSI value.

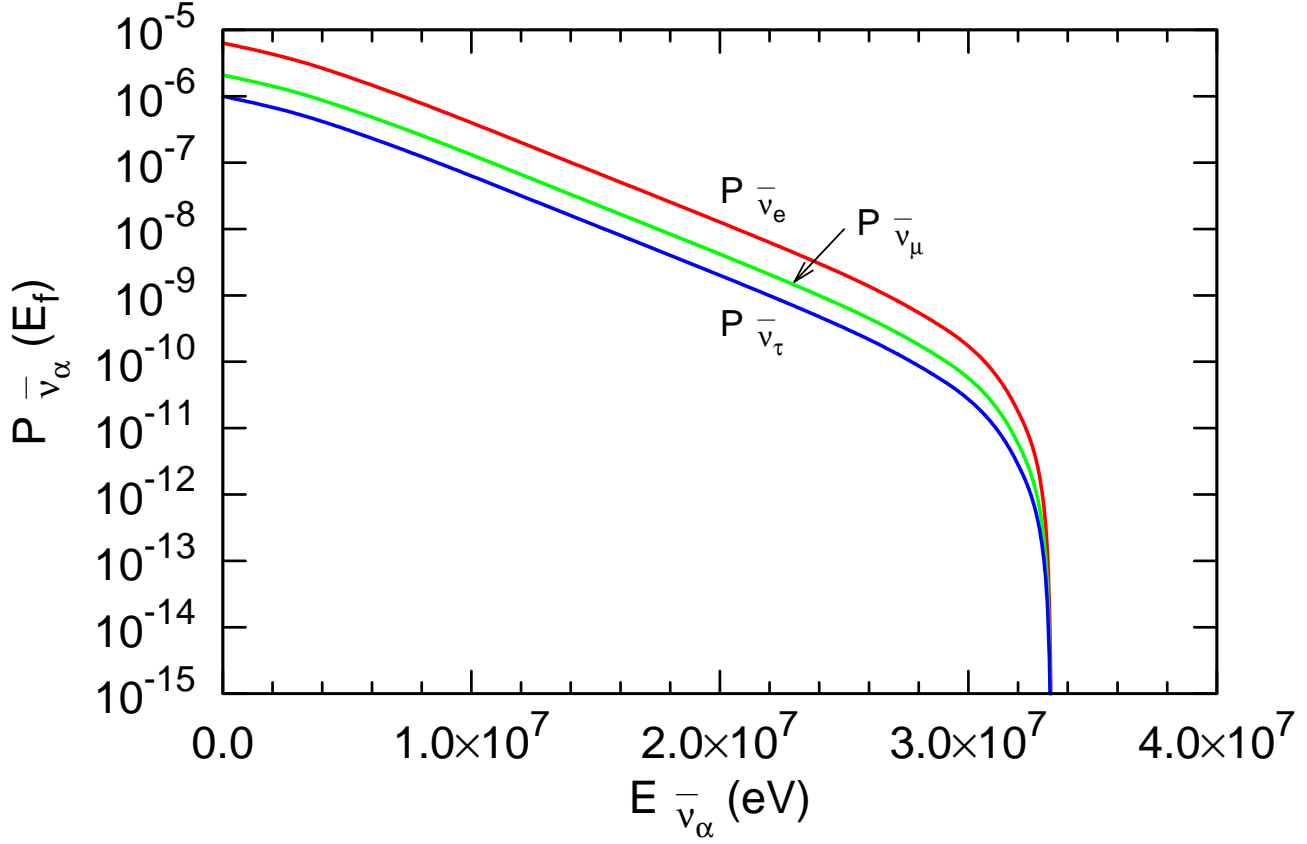


Figure 3: *The antineutrino appearance probabilities from neutrino decay in matter through NSI. The upper bound (22) (the strictest) was used as a common value for the neutrino majoron couplings. Antineutrinos from neutrino decay in supernova matter cannot be detected even if the more conservative bound (32) is used.*